Two-Channel Extended Kalman Filtering
with Intermittent Measurements*

Vicu-Mihalis Maer[1], Zsófia Lendek[1], Ştefan Pîrje[1], Domagoj Tolić[2],
Antun Đuraš[3], Vicko Prkačin[3], Ivana Palunko[3], and Lucian Buşoniu[1]

Abstract— We consider two nonlinear state estimation problems in a setting where an extended Kalman filter receives measurements from two sets of sensors via two channels (2C). In the *stochastic-2C* problem, the channels drop measurements stochastically, whereas in *2C scheduling*, the estimator chooses when to read each channel. In the first problem, we generalize linear-case 2C analysis to obtain – for a given pair of channel arrival rates – boundedness conditions for the trace of the error covariance, as well as a worst-case upper bound. For scheduling, an optimization problem is solved to find arrival rates that balance low channel usage with low trace bounds, and channels are read deterministically with the expected periods corresponding to these arrival rates. We validate both solutions in simulations for linear and nonlinear dynamics; as well as in a real experiment with an underwater robot whose position is being intermittently found in a UAV camera image.

I. INTRODUCTION

The notion of intermittent information, whether an intrinsic or human-imposed control system property, has been extensively investigated for over two decades [1]–[3]. These efforts naturally fall within the scope of networked control systems [4], [5]. For example, lossy communication channels with limited bandwidths, scheduling protocols, packet collisions, sensor occlusions and limited communication/sensing ranges give rise to intermittent information. On the other hand, feedback is expected to supply estimators and controllers with up-to-date data regarding the process of interest. To resolve this tension, it is important to establish conditions leading to a satisfactory estimation and/or control performance in the presence of intermittent information. Herein, we focus on estimation under intermittent measurements.

In particular, we consider a scenario in which a nonlinear system is observed by two sets of sensors via two respective channels. Either set of sensors may in general be local, but we use the name "channel" even in that case, since it is standard [6]. Our main objective is to propose solutions for two related problems in this nonlinear two-channel (2C) setting: *stochastic-2C estimation*, where the two channels drop measurements stochastically with different probabilities (an intrinsic property), and *2C scheduling*, in which the estimation algorithm may choose whether to use either of these channels at each discrete time step (a human-imposed property).

The scenario above is motivated by a practical problem that occurs in the European Horizon 2020 SeaClear project [7]. An Unmanned Underwater Vehicle (UUV) has access to its internal sensors at every step, but these sensors cannot compensate for drift in the position estimate. On the other hand, underwater absolute position sensors are expensive and sometimes unreliable, so instead, the UUV position is determined using the camera image of an Unmanned Aerial Vehicle (UAV), which is however possible only when the UUV is close enough to the surface to be visible. Thus, this second sensor is available intermittently, and the UUV chooses when to resurface to make it available. Beyond this specific case, the two-channel (2C) scenario appears e.g. when shared communication networks with limited throughput are encountered [3], [5].

In linear Kalman filtering with intermittent measurements on a single channel, conditions on the boundedness of estimation error covariance were developed in [8]. That reference showed that there exists a critical value for the arrival rate of the single-channel measurements, beyond which the covariance becomes unbounded. This critical probability has been further analyzed in [9]. Reference [6] extended the results in [8] to stochastic-2C Kalman filtering, with probabilities λ_1 and λ_2 of successfully delivering measurements. The authors of [6] proved the existence of a sharp transition curve for the stability of the iteration on the covariance matrices and show that, when one of the arrival probabilities is fixed, the critical value of the other one can be found by solving a series of linear matrix inequality (LMI) feasibility problems. In the previous works, the arrival probabilities were assumed to be i.i.d. from a Bernoulli distribution. The case when the observations become available according to a Markov process modelling a Gilbert-Elliot channel has been considered in [10].

As a first contribution, we "turn around" the estimation method from [6] so as to apply it to *linear 2C scheduling*. To this end, we read each channel $i \in \{1, 2\}$ with period $T_i = \lfloor \frac{1}{\lambda_i} \rfloor$,[1] which ensures that the guarantees of [6] apply with the corresponding values of λ_i. To find a pair of arrival rates (λ_1, λ_2), we optimize over a predefined set of candidate pairs

[1]Vicu-Mihalis Maer, Zsófia Lendek, Ştefan Pîrje, and Lucian Buşoniu are with the Technical University of Cluj-Napoca, Cluj-Napoca, Romania {vicu.maer, zsofia.lendek, stefan.pirje}@aut.utcluj.ro, lucian@busoniu.net

[2]Domagoj Tolić is with RIT Croatia, Dubrovnik, Croatia domagoj.tolic@croatia.rit.edu

[2]Antun Đuraš, Vicko Prkačin, and Ivana Palunko are with the University of Dubrovnik, Dubrovnik, Croatia {antun.djuras, vicko.prkacin, ivana.palunko}@unidu.hr

[1]Operator $\lfloor \cdot \rfloor$ takes the floor of the argument.

from which we exclude infeasible values that lead to unstable estimates. The objective function balances low values of λ_i, so as to reduce channel usage, with a low trace of the error covariance matrix, so as to improve estimation accuracy.

Our larger objective is to devise a solution for the nonlinear case, which will be the key contribution of the paper and the main difference from [6]. For that purpose, we first analyze *stochastic-2C* Extended Kalman Filtering (EKF) for a class of discrete-time nonlinear systems in which the linearized transition dynamics vary in a polytope. For a given pair of arrival rates, we develop LMI conditions to establish boundedness of the covariance matrices and compute a worst-case upper bound. To our best knowledge, the present paper is the first to consider the nonlinear 2C setting. Stochastic stability of the discrete-time EKF has been investigated in [11], and the case with intermittent measurements on a *single* channel has been analyzed in [12]–[14]. While the discrete-time model considered in [12] is quite general, it has the shortcoming that the measurement matrix, albeit time-varying, must be invertible. Specific variants of EKF with intermittent measurements have been developed for localization [15] and tracking [16]–[18]. Stability of the unscented Kalman filter with intermittent observations has been analyzed in [19].

Moreover, we consider *2C scheduling* for the EKF, where we solve a similar optimization problem to the one from the linear case in order to get λ_i, and then read the channels with the corresponding periods T_i. Differently from the linear case, we apply the newly developed EKF conditions. Since this solution may sometimes be conservative, we additionally propose an empirical, iterative application of the KF conditions, which assumes that the nonlinear dynamics are slowly varying. This last approach linearizes the nonlinear system around the current operating point and recomputes λ_i by solving the linear-case optimization problem. The procedure is repeated when the dynamics deviate significantly from the previous linearization.

To illustrate the approaches developed, we start with simulations in the linear KF case, since the approach in [6] was not validated numerically. Then, we apply 2C scheduling to estimate the pose of a nonlinear rigid-body system using an EKF. Finally, we present a real-life underwater robotics experiment where the onboard-channel is always on, and the UAV-camera-based positioning channel is read with our 2C-scheduling approach. In this experiment, the state estimate is validated against underwater acoustic positioning.

Next, in Section II, we provide the analysis of the stochastic 2C EKF, followed by the methods for 2C scheduling in both the linear and nonlinear cases in Section III. Simulation and real-robot experimental results are given in Sections IV and V, respectively. Section VI concludes the paper.

II. ANALYSIS OF STOCHASTIC-2C EXTENDED KALMAN FILTERING

The main theoretical contribution of the paper is to analyze the statistical properties of the covariance matrices for the EKF, when applied to a class of discrete-time nonlinear systems with intermittent 2C measurements.

We consider the discrete-time nonlinear system

$$
\begin{aligned}
\boldsymbol{x}_{k+1} &= f(\boldsymbol{x}_k) + B\boldsymbol{u}_k + w_k, \\
\boldsymbol{y}_k &= C\boldsymbol{x}_k + v_k,
\end{aligned}
\tag{1}
$$

where $\boldsymbol{x}_k \in \mathcal{R}^{n_x}$ denotes the state at time k, $\boldsymbol{u} \in \mathcal{R}^{n_u}$ is the input, $\boldsymbol{y} \in \mathcal{R}^{n_y}$ is the measured output, and w and v are zero-mean white noises, with covariances $Q = Q^T > 0$ and $R = R^T > 0$, respectively. B is the input matrix and $f : \mathcal{R}^n \to \mathcal{R}^n$ is a vector function. Note that a linear input dependence is assumed.

We consider a scenario similar to [6], with the measurement vector $\boldsymbol{y}$ supplied by two sets of sensors, whose outputs are encoded separately and sent via two different channels. The output $\boldsymbol{y}$ is consequently partitioned as

$$
\begin{pmatrix} \boldsymbol{y}_{k,1} \\ \boldsymbol{y}_{k,2} \end{pmatrix} = \begin{pmatrix} C_1 \\ C_2 \end{pmatrix} \boldsymbol{x}_k + \begin{pmatrix} v_{k,1} \\ v_{k,2} \end{pmatrix}
\tag{2}
$$

with $\boldsymbol{y}_k = \begin{pmatrix} \boldsymbol{y}_{k,1} \\ \boldsymbol{y}_{k,2} \end{pmatrix}$, $C = \begin{pmatrix} C_1 \\ C_2 \end{pmatrix}$, $v_k = \begin{pmatrix} v_{k,1} \\ v_{k,2} \end{pmatrix}$. The measurement noises are $v_{1,k} \sim N(0, R_{11})$ and $v_{2,k} \sim N(0, R_{22})$, where $R = \begin{pmatrix} R_{11} & R_{12} \\ R_{21} & R_{22} \end{pmatrix}$. The channels may be lossy and not all measurement packages are received. The arrival of measurement $\boldsymbol{y}_{k,i}$, $i = 1, 2$, at time k is given by a binary variable, $\gamma_{k,i}$, sampled from a Bernoulli process with probability $P(\gamma_{k,i} = 1) = \lambda_i$, $i = 1, 2$. We consider independent sensors and channels, so the probability of both measurements arriving at the same time is $\lambda_1 \lambda_2$.

To estimate the states of the system, we consider an EKF. We denote $A_k := \frac{\partial f}{\partial \boldsymbol{x}}|_{\widehat{\boldsymbol{x}}_{k|k}}$ and develop general results. Later on, to obtain conditions that are easier to implement, we will consider the case when $A_k \in \mathrm{Co}(\mathcal{A}_j)$, $j = 1, 2, \cdots, a$, where $\mathrm{Co}(.)$ denotes the convex hull.

The time update is independent of the measurements and the predictions are based on model (1), i.e.,

$$
\begin{aligned}
\widehat{\boldsymbol{x}}_{k+1|k} &= f(\widehat{\boldsymbol{x}}_{k|k}) + B\boldsymbol{u}_k, \\
P_{k+1|k} &= A_k P_{k|k} A_k^T + Q,
\end{aligned}
\tag{3}
$$

where the usual notations are used, i.e., $k + 1|k$ denotes prediction and so $\widehat{\boldsymbol{x}}_{k+1|k}$ is the predicted state, $\widehat{\boldsymbol{x}}_{k|k}$ is the estimated state after the kth measurement has been processed, $P_{k|k}$ is the estimator covariance matrix at the same moment, and so on.

Following [6], [8], the update equations depend on the measurements received. If no measurements are received, then only prediction is performed. Otherwise, the state and the covariance matrices are updated using the received measurements, i.e.,

$$
\begin{aligned}
\widehat{\boldsymbol{x}}_{k+1|k+1} &= \widehat{\boldsymbol{x}}_{k+1|k} + \\
&+ \gamma_{k+1,1}\gamma_{k+1,2} P_{k+1|k} C^T (CP_{k+1|k}C^T + R)^{-1} \times \\
&\times (\boldsymbol{y}_{k+1} - C\widehat{\boldsymbol{x}}_{k+1|k}) \\
&+ \gamma_{k+1,1}(1 - \gamma_{k+1,2}) P_{k+1|k} C_1^T (C_1 P_{k+1|k} C_1^T + R_{11})^{-1} \times \\
&\times (\boldsymbol{y}_{k+1,1} - C_1\widehat{\boldsymbol{x}}_{k+1|k})
\end{aligned}
$$

$$+ (1 - \gamma_{k+1,1})\gamma_{k+1,2}P_{k+1|k}C_2^T(C_2P_{k+1|k}C_2^T + R_{22})^{-1} \times$$
$$\times (\boldsymbol{y}_{k+1,2} - C_2\widehat{\boldsymbol{x}}_{k+1|k}),$$
$$P_{k+1|k+1} = P_{k+1|k} -$$
$$- \gamma_{k+1,1}\gamma_{k+1,2}P_{k+1|k}C^T(CP_{k+1|k}C^T + R)^{-1}CP_{k+1|k}$$
$$- \gamma_{k+1,1}(1 - \gamma_{k+1,2})P_{k+1|k}C_1^T(C_1P_{k+1|k}C_1^T + R_{11})^{-1} \times$$
$$\times C_1 P_{k+1|k}$$
$$- (1 - \gamma_{k+1,1})\gamma_{k+1,2}P_{k+1|k}C_2^T(C_2P_{k+1|k}C_2^T + R_{22})^{-1} \times$$
$$\times C_2 P_{k+1|k}. \tag{4}$$

In what follows, we use the simplified notation $P_{k+1} := P_{k+1|k}$. Then, the predicted covariance matrix at sample $k+1$ can be expressed as

$$P_{k+1} = A_k P_k A_k^T + Q -$$
$$- \gamma_{k,1}\gamma_{k,2}A_k P_k C^T(CP_kC^T + R)^{-1}CP_kA_k^T$$
$$- \gamma_{k,1}(1 - \gamma_{k,2})A_k P_k C_1^T(C_1P_kC_1^T + R_{11})^{-1}C_1P_kA_k^T$$
$$- (1 - \gamma_{k,1})\gamma_{k,2}A_k P_k C_2^T(C_2P_kC_2^T + R_{22})^{-1}C_2P_kA_k^T. \tag{5}$$

Remark 1: Note that contrary to the linear case, the matrices P_k, $P_{k+1|k}$ are not the error covariance matrices. However, for simplicity, we will refer to them as such. Furthermore, since measurements may be lost, both $\widehat{\boldsymbol{x}}$ and P become random variables (as they depend on the random variables γ_1 and γ_2).

In this setting, our goal is to determine conditions on the existence of an upper bound on the covariance matrices P_k, given the arrival probabilities λ_1 and λ_2 of the measurements; and to determine the minimal arrival probabilities λ_1 and λ_2 such that the covariance matrices remain bounded. In order to do this, we exploit and generalize some of the results presented in [6] and [8]. Similar to the mentioned results, we define the functions:

$$g_{\lambda_1\lambda_2}(k, X) := A_k X A_k^T + Q -$$
$$- \lambda_1\lambda_2 A_k X C^T(CXC^T + R)^{-1}CXA_k^T$$
$$- \lambda_1(1 - \lambda_2)A_k X C_1^T(C_1XC_1^T + R_{11})^{-1}C_1XA_k^T$$
$$- (1 - \lambda_1)\lambda_2 A_k X C_2^T(C_2XC_2^T + R_{22})^{-1}C_2XA_k^T \tag{6}$$

and

$$\phi(k, K_k, K_{k,1}, K_{k,2}, X) :=$$
$$(1 - \lambda_1)(1 - \lambda_2)(A_k X A_k^T + Q) + \lambda_1\lambda_2(F_k X F_k^T + V_k)$$
$$+ \lambda_1(1 - \lambda_2)(F_{k,1}X F_{k,1}^T + V_{k,1})$$
$$+ (1 - \lambda_1)\lambda_2(F_{k,2}X F_{k,2}^T + V_{k,2}), \tag{7}$$

where $F_k = A_k + KC$, $F_{k,1} = A_k + K_{k,1}C_1$, $F_{k,2} = A_k + K_{k,2}C_2$, $V_k = Q + K_k R K_k^T$, $V_{k,1} = Q + K_{k,1}R_{11}K_{k,1}^T$, $V_{k,2} = Q + K_{k,2}R_{22}K_{k,2}^T$, and $X \geq 0$. We also define $K_{k,x} = -A_k X C^T(CXC^T + R)^{-1}$, $K_{k,1,x} = -A_k X C_2^T(C_1XC_1^T + R_{11})^{-1}$, $K_{k,2,x} = -A_k X C_2^T(C_2XC_2^T + R_{22})^{-1}$.

It is straightforward to see that in the linear case, when A_k is constant, the problem reduces to that in [6]. Furthermore, for a fixed k, the properties in [6] and Lemmas 1 and 2 in [8] hold. Specifically, for any given k,

we have that $E(P_{k+1}|P_k) = g_{\lambda_1\lambda_2}(k, P_k)$, $g_{\lambda_1\lambda_2}(k, X)$ is concave and non-decreasing in X, $g_{\lambda_1\lambda_2}(k, X) \geq (1 - \lambda_1)(1 - \lambda_2)A_k X A_k^T + Q$, and thus it is possible to obtain a lower bound on $E(g_{\lambda_1\lambda_2}(k, P_k))$. Furthermore, with the definitions of $K_{k,x}$, $K_{k,1,x}$, and $K_{k,2,x}$, it follows that $\phi(k, K_{k,x}, K_{k,1,x}, K_{k,2,x}, X) = \min_{K_{k,x}, K_{k,1,x}, K_{k,2,x}} \phi(k, K_k, K_{k,1}, K_{k,2}, X)$.

Next, we state some lemmas that will be useful for developing the boundedness conditions.

Lemma 1: Define the operator

$$\mathcal{L}(k, Y) := (1 - \lambda_1)(1 - \lambda_2)(A_k Y A_k^T) + \lambda_1\lambda_2 F_k Y F_k^T$$
$$+ \lambda_1(1 - \lambda_2)F_{k,1}Y F_{k,1}^T + (1 - \lambda_1)\lambda_2 F_{k,2}Y F_{k,2}^T. \tag{8}$$

$\mathcal{L}(k, Y)$ is linear in Y and $\mathcal{L}(k, Y) \geq 0$. Assume that there exists $\bar{Y} > 0$ such that $\bar{Y} > \mathcal{L}(k, \bar{Y})$, $\forall k$. Then,
1) $\forall W \geq 0$, $\lim_{k\to\infty} \mathcal{L}(k, W) = 0$.
2) Let $U_k \geq 0$ bounded and consider $Y_{k+1} = \mathcal{L}(k, Y_k) + U_k$ initialized at Y_0. Then, the sequence Y_k is bounded.

Proof: Based on the assumption that $\exists \bar{Y} > 0$ so that $\bar{Y} > \mathcal{L}(k, \bar{Y})$, $\forall k$, one can choose $0 \leq r < 1$ so that $\mathcal{L}(k, \bar{Y}) < r\bar{Y}$, $\forall k$. The rest of the proof follows the same lines as that of Lemma 3 in [8]. ∎

Lemma 2: Consider the operator $\phi(k, K, K_1, K_2, X)$ defined in (7). If there exist matrices K_k, $K_{k,1}$, $K_{k,2}$, and $\bar{P} > 0$ so that $\bar{P} > \phi(k, K_k, K_{k,1}, K_{k,2}, \bar{P})$, then the sequence $P_{k+1} = g_{\lambda_1,\lambda_2}(k, P_0)$ is bounded for any P_0.

Proof: Define the matrices $F_k = A_k + K_k C$, $F_{k,1} = A_k + K_{k,1}C$, and $F_{k,2} = A_k + K_{k,2}C$ and consider the operator $\mathcal{L}(k, Y)$ defined in (8). It is easy to verify that $\phi(k, K_k, K_{k,1}, K_{k,2}, X) = \mathcal{L}(k, X) + (1 - \lambda_1)(1 - \lambda_2)Q + \lambda_1\lambda_2 V_k + \lambda_1(1 - \lambda_2)V_{k,1} + (1 - \lambda_1)\lambda_2 V_{k,2}$, where $V_k = Q + K_k R K_k^T$, $V_{k,1} = Q + K_{k,1}R_{11}K_{k,1}^T$, $V_{k,2} = Q + K_{k,2}R_{22}K_{k,2}^T$, i.e., $\phi(k, K_k, K_{k,1}, K_{k,2}, X) = \mathcal{L}(k, X) + U_k$, with U_k being defined as $U_k = (1 - \lambda_1)(1 - \lambda_2)Q + \lambda_1\lambda_2 V_k + \lambda_1(1 - \lambda_2)V_{k,1} + (1 - \lambda_1)\lambda_2 V_{k,2}$ and, since $Q > 0$, $R > 0$, $R_{11} > 0$, $R_{22} > 0$, $U_k > 0$. Using the assumption that $\bar{P} > \phi(k, K_k, K_{k,1}, K_{k,2}, \bar{P})$, we have $\bar{P} > \mathcal{L}(k, \bar{P}) + U_k > \mathcal{L}(k, \bar{P})$.

On the other hand, we also have $P_{k+1} = g_{\lambda_1\lambda_2}(k, P_k) \leq \phi(k, K_k, K_{k,1}, K_{k,2}, P_k) = \mathcal{L}(k, P_k) + U_k$. Based on Lemma 1, the sequence P_k is bounded. ∎

We are now ready to state the main result on the boundedness of the covariance matrices:

Theorem 1: Consider the operator $\phi(k, K_k, K_{k,1}, K_{k,2}, X)$ defined in (7). Assume that there exist matrices K_k, $K_{k,1}$, $K_{k,2}$ and a positive matrix $P = P^T > 0$ so that $P > \phi(k, K_k, K_{k,1}, K_{k,2}, P)$. Then, for any initial condition $P_0 \geq 0$, $\lim_{k\to\infty} P_k = \lim_{k\to\infty} g_{\lambda_1\lambda_2}(k, P_0)$ is bounded.

Remark 2: Contrary to the results in [6], [8], a single point of transition or a transition curve between boundedness and unboundedness of P_k in general will not exist. However, a worst-case upper bound on the critical probabilities λ_1 and λ_2 can be computed similarly to Theorem 2 of [6].

If (λ_1, λ_2) is such that boundedness is maintained, a limit on the bound of P_k is given by the following theorem:

Theorem 2: Assume that (A_k, Q) is controllable, (A_k, C) is detectable $\forall k$ and the pair (λ_1, λ_2) is such that P_k is bounded. Then, $\lim_{k\to\infty} P_k \leq V$, where $V > g_{\lambda_1\lambda_2}(k, V)$, $V > 0$, $\forall k$.

Proof: Follows the lines of Theorem 6 in [8], taking into account that $V > 0$ and $V > g_{\lambda_1\lambda_2}(k, V)$ have to hold $\forall k$. ∎

Next, we formulate a theorem to compute a worst-case upper bound on the probabilities.

Theorem 3: If (A_k, Q) is controllable, (A_k, C) is detectable $\forall k$, then the following statements are equivalent:

1) there exists $\bar{X} > 0$ such that $\bar{X} > g_{\lambda_1\lambda_2}(k, \bar{X})$, $\forall k$,
2) there exist K_k, $K_{k,1}$, $K_{k,2}$ and $\bar{X} > 0$ so that $\bar{X} > \phi(k, K_k, K_{k,1}, K_{k,2}, \bar{X})$, $\forall k$,
3) there exist $\bar{Z}_k$, $\bar{Z}_{k,1}$, $\bar{Z}_{k,2}$, and $0 < \bar{Y} \leq I$ such that $\forall k$

$$\Psi_k = \begin{pmatrix} Y & \sqrt{\lambda_1\lambda_2}(YA_k + Z_kC) & \Psi_{13} & \Psi_{14} \\ (*) & Y & 0 & 0 \\ (*) & (*) & Y & 0 \\ (*) & (*) & (*) & Y \end{pmatrix} > 0, \tag{9}$$

where $\Psi_{13} = \sqrt{\lambda_1(1-\lambda_2)}(YA_k + Z_{k,1}C_1)$, $\Psi_{14} = \sqrt{\lambda_2(1-\lambda_1)}(YA_k + Z_{k,2}C_2)$ and $(*)$ denotes the symmetric term.

The condition formulated in (9) is bilinear, due to having to search for λ_1, λ_2, Y, etc. However, if either λ_1 or λ_2 is fixed, then bisection can be used to find the other probability, i.e., one will have to solve a set of LMI feasibility problems. Once a suitable pair (λ_1, λ_2) is found, an upper bound on the matrix P_k can be computed as in the next theorem.

Theorem 4: If there exist $\bar{Z}_k$, $\bar{Z}_{k,1}$, $\bar{Z}_{k,2}$ and $0 < \bar{Y} \leq I$ such that (9) is satisfied, then an upper bound on $\lim_{k\to\infty} g_{\lambda_1\lambda_2}(k, V)$ can be found by solving

$$\text{argmax}_V \text{Trace}(V)$$
$$\text{subject to } V > 0, \Gamma(V) \geq 0 \tag{10}$$

where

$$\Gamma(V) = \begin{pmatrix} A_k V A_k^T + Q - V & \sqrt{\lambda_1\lambda_2}A_k V C^T & \Gamma_{13} & \Gamma_{14} \\ (*) & CVC^T + R & 0 & 0 \\ (*) & (*) & \Gamma_{33} & 0 \\ (*) & (*) & (*) & \Gamma_{44} \end{pmatrix} \tag{11}$$

$\Gamma_{13} = \sqrt{\lambda_1(1-\lambda_2)}A_k V C_1^T$, $\Gamma_{14} = \sqrt{\lambda_2(1-\lambda_1)}A_k V C_2^T$, $\Gamma_{33} = C_1 V C_1^T + R_{11}$, $\Gamma_{44} = C_2 V C_2^T + R_{22}$.

In the developments so far we have considered that the state matrices A_k vary in time without any further constraints. This means that the number of conditions to be solved for Theorems 3 and 4, respectively, is infinite. In practice, however, a domain (possibly overestimated) in which the matrices vary can usually be determined, e.g., by applying sector nonlinearity [20] to the expressions of $\frac{\partial f}{\partial x} x$. Therefore, in what follows, we impose the following assumption.

Assumption 1: There exist constant matrices $\mathcal{A}_j$, and functions $h_j(\cdot)$, $h_j(k) \geq 0$, $\sum_{j=1}^{a} h_j(k) = 1$ so that $A_k \in \text{Co}(\mathcal{A}_j)$, $j = 1, 2, \cdots, a$, i.e., each matrix A_k can

be expressed as the convex combination of the matrices $\mathcal{A}_j$, $j = 1, 2, \cdots, a$, $A_k = \sum_{j=1}^{a} h_j(k)\mathcal{A}_j$.

Remark 3: Although Assumption 1 may be conservative, it is an efficient way to reduce the number of conditions to be solved and gives a way to determine a priori worst-case upper bounds on the critical probabilities λ_1 and λ_2.

Under Assumption 1, a sufficient condition for condition (9) to hold is:

Proposition 1: If there exist $\mathcal{Z}_j$, $\mathcal{Z}_{j,1}$, $\mathcal{Z}_{j,2}$ and $0 < \bar{Y} \leq I$ such that $\forall k$

$$\Psi_j^2 = \begin{pmatrix} Y & \sqrt{\lambda_1\lambda_2}(Y\mathcal{A}_j + \mathcal{Z}_jC) & \Psi_{13}^2 & \Psi_{14}^2 \\ (*) & Y & 0 & 0 \\ (*) & (*) & Y & 0 \\ (*) & (*) & (*) & Y \end{pmatrix} > 0 \tag{12}$$

holds for $j = 1, 2, \ldots, a$, where $\Psi_{13}^2 = \sqrt{\lambda_1(1-\lambda_2)}(Y\mathcal{A}_j + \mathcal{Z}_{j,1}C_1)$, $\Psi_{14}^2 = \sqrt{\lambda_2(1-\lambda_1)}(Y\mathcal{A}_j + \mathcal{Z}_{j,2}C_2)$, then condition (9) holds.

Proof: Let $Z_k = \sum_{j=1}^{a} h_j(k)\mathcal{Z}_j$, $Z_{k,1} = \sum_{j=1}^{a} h_j(k)\mathcal{Z}_{k,j}$, and $Z_{k,2} = \sum_{j=1}^{a} h_j(k)\mathcal{Z}_{j,2}$. Taking into account that $A_k = \sum_{j=1}^{a} h_j(k)\mathcal{A}_j$, $\Psi_k = \sum_{j=1}^{a} h_j(k)\Psi_j^2$. Since $h_j(k) \geq 0$ and $\sum_{j=1}^{a} h_j(k) = 1$, $\Psi_j^2 > 0$, $j = 1, 2, \ldots, a$, that implies $\Psi_k > 0$. □ ∎

A sufficient condition for Theorem 4 is formulated as follows:

Proposition 2: If there exist $\mathcal{Z}_j$, $\mathcal{Z}_{j,1}$, $\mathcal{Z}_{j,2}$, $j = 1, 2, \ldots, a$, and $0 < \bar{Y} \leq I$ such that (12) is satisfied, then an upper bound on $\lim_{k\to\infty} g_{\lambda_1\lambda_2}(k, V)$ can be found solving

$$\text{argmax}_V \text{Trace}(V)$$
$$\text{subject to } V > 0, \Gamma^2(V) \geq 0, j = 1, 2, \ldots, a \tag{13}$$

where

$$\Gamma^2(V) = \begin{pmatrix} \mathcal{A}_j + \mathcal{A}_j^T + Q - V & \sqrt{\lambda_1\lambda_2}\mathcal{A}_j V C^T & \Gamma_{13}^2 & \Gamma_{14}^2 & I \\ (*) & CVC^T + R & 0 & 0 & 0 \\ (*) & (*) & \Gamma_{33}^2 & 0 & 0 \\ (*) & (*) & (*) & \Gamma_{44}^2 & 0 \\ (*) & (*) & (*) & (*) & V \end{pmatrix} \tag{14}$$

$\Gamma_{13}^2 = \sqrt{\lambda_1(1-\lambda_2)}\mathcal{A}_j V C_1^T$, $\Gamma_{14}^2 = \sqrt{\lambda_2(1-\lambda_1)}\mathcal{A}_j V C_2^T$, $\Gamma_{33}^2 = C_1 V C_1^T + R_{11}$, $\Gamma_{44}^2 = C_2 V C_2^T + R_{22}$.

Proof: Recall that $\forall k$, $A_k = \sum_{j=1}^{a} h_j(k)\mathcal{A}_j$. Note that $A_k V A_k^T \geq A_k + A_k^T - V^{-1}$, thus

$$\begin{pmatrix} A_k V A_k^T + Q - V & \sqrt{\lambda_1\lambda_2}A_k V C^T & \Gamma_{13} & \Gamma_{14} \\ (*) & CVC^T + R & 0 & 0 \\ (*) & (*) & \Gamma_{33} & 0 \\ (*) & (*) & (*) & \Gamma_{44} \end{pmatrix} \geq$$

$$\begin{pmatrix} A_k + A_k^T + Q - V - V^{-1} & \sqrt{\lambda_1\lambda_2}A_k V C^T & \Gamma_{13} & \Gamma_{14} \\ (*) & CVC^T + R & 0 & 0 \\ (*) & (*) & \Gamma_{33} & 0 \\ (*) & (*) & (*) & \Gamma_{44} \end{pmatrix}.$$

Applying a Schur complement on the element $A_k + A_k^T + Q - V - V^{-1}$ and taking into account that $A_k = \sum_{j=1}^{a} h_j(k)\mathcal{A}_j$, $\forall k$, we obtain (14). □ ∎

Remark 4: The conditions stated in Propositions 1 and 2 may in some cases be overly conservative as, if satisfied, they will guarantee boundedness and determine an upper bound, respectively, for all the nonlinear systems in the polytope.

Remark 5: It can easily be seen that the conditions in Propositions 1 and 2 reduce to those in Theorems 5 and 6 in [6] in the case of a constant state matrix, i.e., when $A_k = A$, $\forall k$ or $\mathcal{A}_j = A$, $j = 1, 2, \ldots, a$. Specifically, condition (12) reduces to

$$\Psi^l = \begin{pmatrix} Y & \sqrt{\lambda_1 \lambda_2}(YA + ZC) & \Psi_{13}^l & \Psi_{14}^l \\ (*) & Y & 0 & 0 \\ (*) & (*) & Y & 0 \\ (*) & (*) & (*) & Y \end{pmatrix} > 0 \quad (15)$$

with $\Psi_{13}^l = \sqrt{\lambda_1(1 - \lambda_2)}(YA + Z_1C_1)$, $\Psi_{14}^l = \sqrt{\lambda_2(1 - \lambda_1)}(YA + Z_2C_2)$ and the bound on the covariance can be calculated by solving

$$\begin{aligned} &\mathrm{argmax}_V \mathrm{Trace}(V) \\ &\text{subject to } V > 0, \Gamma^l(V) \geq 0, j = 1, 2, \ldots, a \end{aligned} \quad (16)$$

where

$$\Gamma^l(V) = \begin{pmatrix} AVA^T + Q & \sqrt{\lambda_1 \lambda_2}AVC^T & \Gamma_{13}^l & \Gamma_{14}^l \\ (*) & CVC^T + R & 0 & 0 \\ (*) & (*) & \Gamma_{33}^2 & 0 \\ (*) & (*) & (*) & \Gamma_{44}^l \end{pmatrix} \quad (17)$$

$\Gamma_{13}^l = \sqrt{\lambda_1(1 - \lambda_2)}AVC_1^T$, $\Gamma_{14}^l = \sqrt{\lambda_2(1 - \lambda_1)}AVC_2^T$, $\Gamma_{33}^2 = C_1VC_1^T + R_{11}$, $\Gamma_{44}^l = C_2VC_2^T + R_{22}$. Furthermore, if only a single intermittent-measurement channel is considered, the conditions become those in Theorems 5 and 6 in [8].

III. TWO-CHANNEL SCHEDULING

Moving now to the 2C scheduling problem, a straightforward way to solve it is to find a pair of arrival rates (λ_1, λ_2) that satisfy (12) and therefore ensure boundedness of the error covariance matrix; and then to read each channel $i \in \{1, 2\}$ with period $T_i = \lfloor \frac{1}{\lambda_i} \rfloor$. Since there may be many such pairs, we formulate an optimization problem to select the best one:

$$\min_{(\lambda_1, \lambda_2) \in L \text{ s.t. } (12)} \tau + e^{\frac{1}{1 - \lambda_1}} + e^{\frac{1}{1 - \lambda_2}}, \quad (18)$$

where set L contains finitely many candidate pairs (λ_1, λ_2), and $\tau = \mathrm{Trace}(V^*)$ with V^* being the solution of (13) for the pair (λ_1, λ_2). We take finitely many pairs to be able to solve the optimization problem by enumeration. The objective function (18) aims to minimize both the value of the trace (via its upper bound as a proxy) and the arrival rates (channel usage). The exponential formulas in λ_i are used to induce a preference for low arrival rates whenever possible, in order to reduce network usage. However, a lower rate causes the estimation error to grow, so usage is only reduced subject to the LMI constraint on the error trace.

For 2C scheduling in the linear KF case, we apply a similar procedure, but this time with the conditions of [6]:

$$\min_{(\lambda_1, \lambda_2) \in L \text{ s.t. } (15)} \tau' + e^{\frac{1}{1 - \lambda_1}} + e^{\frac{1}{1 - \lambda_2}}, \quad (19)$$

Algorithm 1 2C EKF scheduling with iterative KF conditions

Input: candidate set L, dynamics f, threshold δ
1: $k_1 \leftarrow -\infty$, $k_2 \leftarrow -\infty$
2: **for** each time step $k \geq 0$ **do**
3:      differentiate f around x_k to find A_k
4:      **if** $k = 0$, or $\Delta A_k \geq \delta$ and $k_{\mathrm{lin}} \leq \max\{k_1, k_2\}$ **then**
5:          solve (19) to obtain (λ_1, λ_2)
6:          $k_{\mathrm{lin}} \leftarrow k$
7:      **if** $k - k_1 \geq \lfloor \frac{1}{\lambda_1} \rfloor$ **then**
8:          measure $y_{1,k}$
9:          $k_1 \leftarrow k$
10:     **if** $k - k_2 \geq \lfloor \frac{1}{\lambda_2} \rfloor$ **then**
11:         measure $y_{2,k}$
12:         $k_2 \leftarrow k$
13:    run EKF prediction
14:    **if** any measurement taken **then**
15:       run EKF update by applying (4) for step k

---

where $\tau' = \mathrm{Trace}(V')$ with V' being the solution of (16).

Since the EKF conditions may sometimes be overly conservative, we also propose an empirical alternative in which we recompute the arrival rates by solving (19), whenever the linearized dynamics deviate by more than a threshold δ compared to the steps when the rates were previously computed. The deviation is measured through the 2-norm of the difference between the state transition matrix of the current linearized dynamics and that of the linearized dynamics at the time of the last recomputation: $\Delta A_k := \|A_k - A_{k_{\mathrm{lin}}}\|$. The extra condition $k_{\mathrm{lin}} \leq \max\{k_1, k_2\}$ ensures that at least one measurement was taken after the last recomputation. After each pair of rates is chosen, measurements via the two channels are read with periods $\lfloor \frac{1}{\lambda_i} \rfloor$ between recomputations.

IV. SIMULATION RESULTS

All the simulations use either a KF or EKF to estimate the states. The models used are discrete-time with sampling period $T_s = 0.05\,\mathrm{s}$, and have the form

$$\begin{aligned} \boldsymbol{x}_{k+1} &= f(\boldsymbol{x}_k) + w_k, \\ \boldsymbol{y}_k &= \begin{bmatrix} C_1 \\ C_2 \end{bmatrix} \boldsymbol{x} + v_k, \end{aligned} \quad (20)$$

with w and v representing Gaussian noises with covariances $1\mathrm{e}{-}4I$ and $1\mathrm{e}{-}2I$ respectively. The simulations are carried out for a duration of $10\,\mathrm{min}$. In every case we check the appropriate LMI conditions for stable estimates and/or desired error covariance bounds. The LMIs are solved using YALMIP [21] with the SeDuMi solver [22].

A. 2C Estimation and Scheduling for a Linear System

In this scenario we find bounds on the error trace for Kalman filtering in the linear case, which as noted reduces to the method in [6]; thus, we provide a numerical validation of that method, which was not done in the original paper. Moreover, we apply our new 2C scheduling procedure in
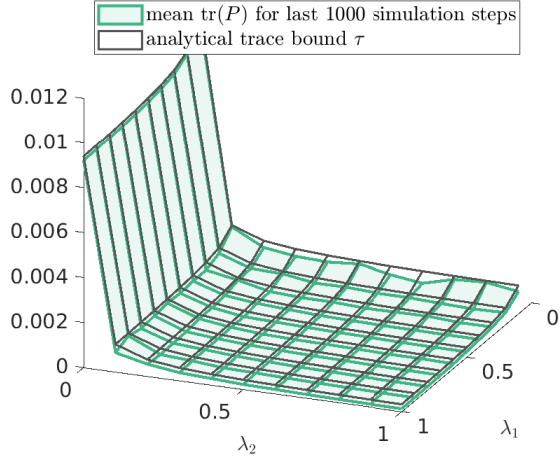
Fig. 1: Analytical bound versus actual trace of the error covariance matrix in simulation.

the linear case. The dynamics model linear one-dimensional motion. Following the structure in (20), $f(\boldsymbol{x}) = A\boldsymbol{x}$ with $A = \begin{bmatrix} 1 & 0.05 \\ 0 & 0.995 \end{bmatrix}$, and $C_1 = \begin{bmatrix} 1 & 0 \end{bmatrix}, C_2 = \begin{bmatrix} 0 & 1 \end{bmatrix}$. The states $\boldsymbol{x}$ consist of the position x and velocity v_x.

The arrival rates vary on a grid $(\lambda_1, \lambda_2) \in L := \{0, 0.1, 0.2, 0.3, 0.4, 0.5, 0.6, 0.7, 0.8, 0.9, 1\}^2$. Figure 1 compares the analytical upper bounds τ' on the trace with the traces obtained in simulation, for all values of λ_i on the grid. The analytical values indeed serve as useful upper bounds for the actual traces: they are always larger, but close in value.
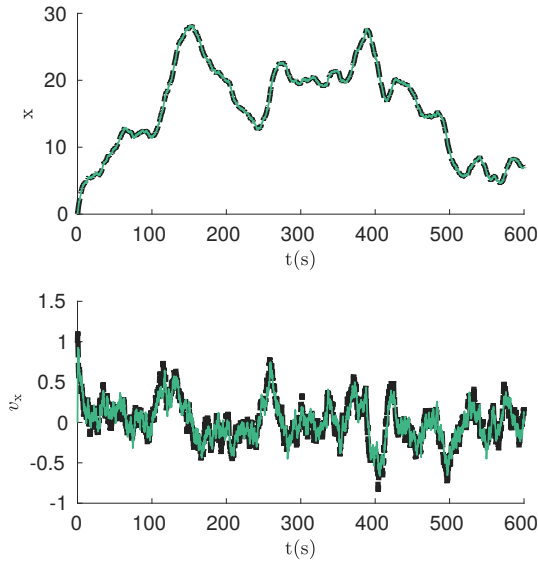

Fig. 2: Real versus KF-estimated trajectories for linear model with sensor scheduling. The black dashed lines represent the states and the teal lines are the estimates.

Next, to solve 2C scheduling, we use (19) to select a

pair (λ_1, λ_2) from the grid. This pair turns out to be $\lambda_1 = 0.1, \lambda_2 = 0$. Note that because the system is observable from the first channel (position), the method chooses to not use the second channel at all. KF results using scheduling with this pair are shown in Figure 2. The analytical trace bound is $113\mathrm{e}{-4}$, whereas the trace in simulation is $101\mathrm{e}{-4}$.

B. 2C Scheduling for Nonlinear Dynamics

In the nonlinear case, the dynamics used comprise a five degree-of-freedom (5-DOF) constant acceleration kinematic model. The degree of freedom removed from the standard 6-DOF model is the pitch angle. This was done partly to control computational complexity and partly because the real UUV for which we will later use these dynamics lacks this degree of freedom. Keeping the structure of (20), the state vector is $\boldsymbol{x} = [x, y, z, \phi, \psi, v_x, v_y, v_z, v_\phi, v_\psi, a_x, a_y, a_z]^T$, and

$$f(\boldsymbol{x}) =$$

$$\boldsymbol{x} + T_s \begin{bmatrix} v_x \cos\psi - v_y \sin\psi \cos\phi + v_z \sin\psi \sin\phi \\ v_x \cos\psi - v_y \sin\psi \cos\phi + v_z \sin\psi \sin\phi \\ v_y \sin\phi + v_z \cos\phi \\ v_\phi \\ v_\psi \cos\phi \\ a_x \\ a_y \\ a_z \\ 0_{5\times 1} \end{bmatrix}, \quad (21)$$

$$C_1 = \begin{bmatrix} 0_{7\times 3} & 1_{7\times 7} \end{bmatrix}, \ C_2 = \begin{bmatrix} 1_{3\times 3} & 0_{3\times 7} \end{bmatrix}.$$

The sector nonlinearity approach is applied to the derivative of f with respect to the state, thereby obtaining the matrices $\mathcal{A}_j$ needed to define the convex hull in which A_k lives and to construct the LMI conditions.

The 2C scheduling problem (18) is solved with $(\lambda_1, \lambda_2) \in L := \{0.001, 0.01, 0.1, 0.5, 0.625\}^2$. The chosen pair is $\lambda_1 = 0.1, \lambda_2 = 0.1$. For this pair, the trajectories of the linear and angular positions and of their respective estimates are shown in Figure 3. The analytical trace bound is 0.3874, whereas the trace in simulation is 0.0936, showing that the conditions are conservative.

This motivates us to perform another simulation, this time using Algorithm 1 to compute the feedback periods for the two channels. The threshold for the deviation of the dynamics of the system is $\delta = 0.1$, chosen experimentally. The state trajectories are very similar to Figure 3, so they are not shown here. Instead, Figure 4 shows the feedback periods chosen along the simulation for both channels, along with the feedback period which corresponds to the single pair $\lambda_1 = 0.1, \lambda_2 = 0.1$ chosen using (18). It is apparent that Algorithm 1 produces less conservative periods, albeit without analytical guarantees. The trace for this simulation is 0.1316.
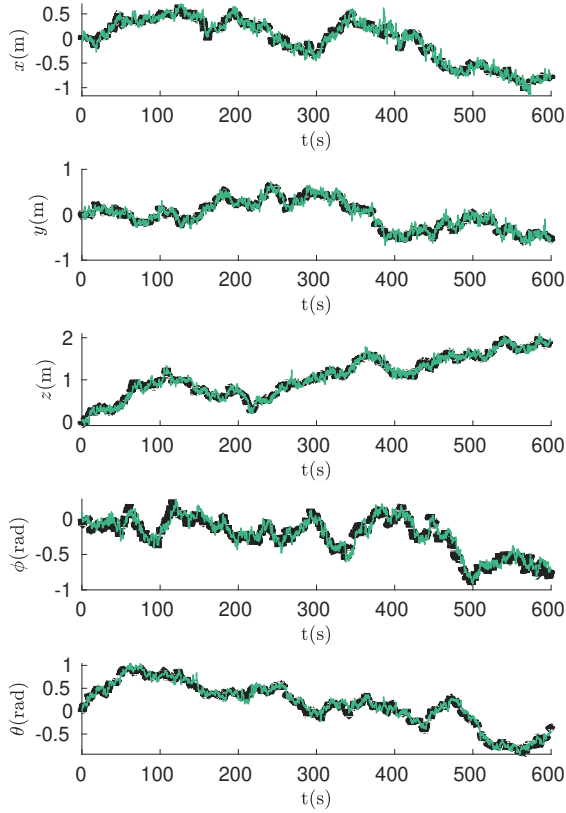
Fig. 3: Linear and angular positions and their estimates for non-linear model with sensor scheduling. The black dashed lines represent the states and the teal lines are the estimates.
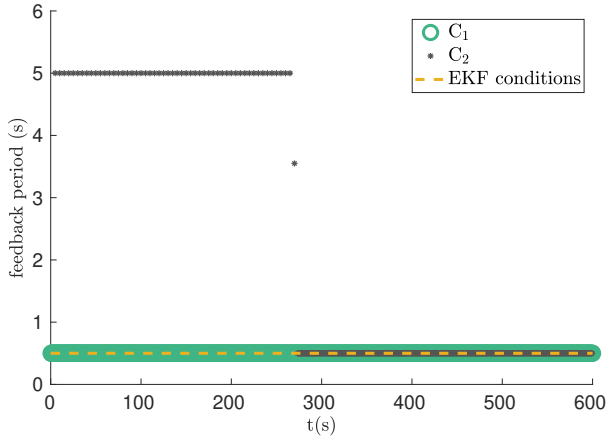

Fig. 4: Feedback periods for 2C scheduling with the non-linear model.

V. EXPERIMENTAL RESULTS FOR AN UNDERWATER ROBOT

Finally, we apply 2C scheduling with real data collected for UUV pose estimation in the SeaClear project [7], see Figure 5. The two channels correspond to the internal and the off-board sensors. Similarly to the non-linear problem of Section IV-B, the UUV measures its angular position and velocity using an inertial measurement unit, and its linear velocity using a Doppler velocity logger. Differently from

the simulated problem, the UUV also has direct access to the measurement of its depth z using a pressure sensor. As a result, the second channel only communicates the position of the UUV in the XY-plane, determined from camera images of a UAV, while the z coordinate is communicated on the first channel.
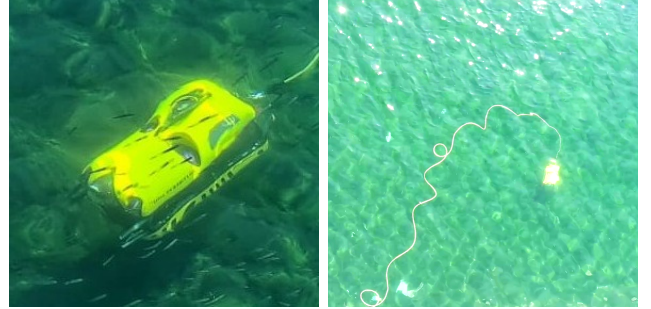

Fig. 5: Left: MiniTortuga, the UUV used for the experiment. Right: Example camera image of the UAV from the collected data set, used to determine the position of the UUV (the image has been cropped for better visibility).

The internal sensors provide feedback at each timestep ($\lambda_1 = 1$) and only the loop closure period for the data sent by the UAV varies. The rate λ_2 is selected from the same set of discrete values as in Section IV-B, $\lambda_2 \in \{0.001, 0.01, 0.1, 0.5, 0.625\}$. The linearized model used is identical to that from the simulations. The EKF is implemented using the robot_localization library [23].

In this experiment, it turns out that irrespective of whether (18) or the iterative Algorithm 1 is applied, the resulting value of λ_2 is always the same: 0.01. Thus, in this case the EKF solution is less conservative than in the simulations, possibly because along this trajectory the angles only rotate the dynamics, without significantly affecting the stability properties of the system.
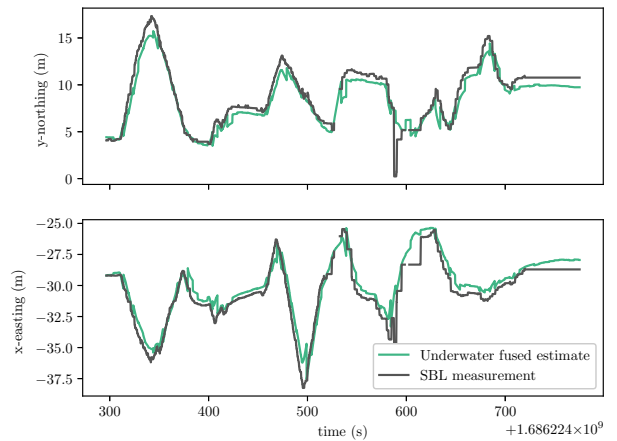

Fig. 6: Estimation results using channel scheduling for the real UUV. The horizontal axis displays Unix epoch time.

Figure 6 compares the positions in the plane estimated

using the EKF with channel scheduling, versus positions read from a short baseline (SBL) acoustic positioning system. The SBL measurement is used as a proxy for the ground truth position of the UUV. It can be seen that the estimated position is close to the one measured by the SBL, with a root mean squared error of $1.3915\,\mathrm{m}$ between the two.

VI. Conclusions

This paper characterized the estimation error for an EKF that reads sensors over two channels that drop measurements stochastically, and proposed a solution to deterministically choose when to read the channels when they are under the control of the estimator. The approaches were validated both in simulations and on real data. To generalize the approach in future work, several interesting directions emerge: allowing for an arbitrary number of channels instead of just two, deriving similar results for the unscented Kalman filter, or taking into account specific scheduling protocols.

References

[1] K. Åström and B. Bernhardsson, "Comparison of Riemann and Lebesgue sampling for first order stochastic systems," in *IEEE Conference on Decision and Control (CDC)*, vol. 2, pp. 2011–2016, 2002.

[2] M. Lemmon, *Event-triggered Feedback in Control, Estimation, and Optimization*, vol. 405 of *Lecture Notes in Control and Information Sciences*. Springer Verlag, 2010.

[3] D. Tolić and S. Hirche, *Networked Control Systems with Intermittent Feedback*. Boca Raton, FL, USA: CRC Press, 2017.

[4] J. Hespanha, P. Naghshtabrizi, and X. Yonggang, "A survey of recent results in Networked Control Systems," *Proceedings of the IEEE*, vol. 95, no. 1, pp. 138 – 162, 2007.

[5] A. Bemporad, M. Heemels, and M. Vejdemo-Johansson, *Networked Control Systems*, vol. 406 of *Lecture Notes in Control and Information Sciences*. Springer-Verlag London, 2010.

[6] X. Liu and A. Goldsmith, "Kalman filtering with partial observation losses," in *2004 43rd IEEE Conference on Decision and Control (CDC) (IEEE Cat. No.04CH37601)*, vol. 4, pp. 4180–4186 Vol.4, 2004.

[7] SeaClear, "Project Website." https://seaclear-project.eu/, 2023.

[8] B. Sinopoli, L. Schenato, M. Franceschetti, K. Poolla, M. Jordan, and S. Sastry, "Kalman filtering with intermittent observations," *IEEE Transactions on Automatic Control*, vol. 49, no. 9, pp. 1453–1464, 2004.

[9] K. Plarre and F. Bullo, "On Kalman filtering for detectable systems with intermittent observations," *IEEE Transactions on Automatic Control*, vol. 54, no. 2, pp. 386–390, 2009.

[10] Y. Mo and B. Sinopoli, "Kalman filtering with intermittent observations: Tail distribution and critical value," *IEEE Transactions on Automatic Control*, vol. 57, no. 3, pp. 677–689, 2012.

[11] K. Reif, S. Gunther, E. Yaz, and R. Unbehauen, "Stochastic stability of the discrete-time Extended Kalman Filter," *IEEE Transactions on Automatic Control*, vol. 44, no. 4, pp. 714–728, 1999.

[12] S. Kluge, K. Reif, and M. Brokate, "Stochastic stability of the Extended Kalman Filter with intermittent observations," *IEEE Transactions on Automatic Control*, vol. 55, no. 2, pp. 514–518, 2010.

[13] G. Wang, J. Chen, and J. Sun, "Stochastic stability of extended filtering for non-linear systems with measurement packet losses," *IET Control Theory & Applications*, vol. 7, no. 17, pp. 2048–2055, 2013.

[14] X. Liu, L. Li, Z. Li, T. Fernando, and H. H. C. Iu, "Stochastic stability condition for the Extended Kalman Filter with intermittent observations," *IEEE Transactions on Circuits and Systems II: Express Briefs*, vol. 64, no. 3, pp. 334–338, 2017.

[15] H. Ahmad and T. Namerikawa, "Extended Kalman filter-based mobile robot localization with intermittent measurements," *Systems Science & Control Engineering*, vol. 1, no. 1, pp. 113–126, 2013.

[16] J. D. Hicks, "Performance comparison of an extended Kalman filter and an iterated extended Kalman filter for orbit determination of space debris with poor apriori information and intermittent observations," Master's thesis, Auburn University, Auburn, Alabama, USA, 2012.

[17] P. Chen, H. Ma, S. Gao, and Y. Huang, "Modified extended Kalman filtering for tracking with insufficient and intermittent observations," *Mathematical Problems in Engineering*, no. 981727, 2015.

[18] J. Shi, Y. Li, G. Qi, and A. Sheng, "Extended target tracking filter with intermittent observations," *IET Signal Processing*, vol. 10, no. 6, pp. 592–602, 2016.

[19] L. Li and Y. Xia, "Stochastic stability of the unscented Kalman filter with intermittent observations," *Automatica*, vol. 48, no. 5, pp. 978–981, 2012.

[20] H. Ohtake, K. Tanaka, and H. Wang, "Fuzzy modeling via sector nonlinearity concept," in *Proceedings of the Joint 9th IFSA World Congress and 20th NAFIPS International Conference*, vol. 1, (Vancouver, Canada), pp. 127–132, July 2001.

[21] J. Löfberg, "Yalmip : A toolbox for modeling and optimization in matlab," in *In Proceedings of the CACSD Conference*, (Taipei, Taiwan), 2004.

[22] J. F. Sturm, "Using sedumi 1.02, a MATLAB toolbox for optimization over symmetric cones," *Optimization Methods and Software*, vol. 11, no. 1-4, pp. 625–653, 1999.

[23] T. Moore and D. Stouch, "A generalized Extended Kalman Filter implementation for the Robot Operating System," in *Intelligent Autonomous Systems 13* (E. Menegatti, N. Michael, K. Berns, and H. Yamaguchi, eds.), (Cham), pp. 335–348, Springer International Publishing, 2016.